# The Viking Orbiter Visual Imaging Subsystem

John B. Wellman,* Frederick P. Landauer,† David D. Norris,‡ and Thomas E. Thorpe§
*Jet Propulsion Laboratory, Pasadena, Calif.*

**A Visual Imaging Subsystem consisting of two slow-scan television cameras forms part of the scientific payload of each of two Viking Orbiter Spacecraft presently photographing the surface of Mars. These cameras are used to evaluate the potential landing sites on Mars, and to conduct other scientific investigations of the planet. The camera system described in this paper was subjected to an extensive test and calibration program prior to launch. Based on this calibration and subsequent analyses, surface resolution exceeding 100 m will be achieved from the periapsis portion of the Viking orbits. The inherent geometric accuracies of the Orbiter cameras surpass those of cameras used in previous planetary missions. The analyses of images acquired during the cruise phase of the mission confirm that the cameras have survived the rigors of launch and are performing in a manner consistent with the prelaunch calibrations.**

## I. Introduction

A 1972 article[1] summarized the scientific objectives of the Orbiter imaging investigation and described the camera design. Since that writing, significant changes in the camera design have occurred. In addition, the cameras have undergone an extensive ground calibration and have been successfully tested in flight. It is therefore appropriate to describe the camera design, calibration, and test results with emphasis on the predicted performance at Mars. A more detailed program of scientific objectives has emerged from analysis of the data from the highly successful Mariner 9 mission and the several years of Viking mission planning activities; however, that subject is not addressed here.

In the early stages of planning for the Viking mission it was recognized that the scientific investigation of the Martian surface and the need for observational data to evaluate and certify potential landing sites required an imaging subsystem capable of providing high-resolution images which could be mosaicked into contiguous coverage of relatively large regions of the surface. To provide contiguous coverage of approximately 100 m resolution from the planned orbits required a camera whose frame time was an order of magnitude shorter than previous Mariner cameras.

To provide coverage at this resolution but wide enough to cover the projected landing error ellipse, two identical cameras with offset pointing were needed. These basic requirements for coverage and resolution determined the instrument design parameters of focal length, frame size, frame time, and data rate.

## II. Visual Imaging Subsystem Description

To meet the joint requirements of coverage and resolution, several departures from previous Mariner camera designs were necessitated. New, diffraction limited optics of 475 mm focal length were employed. The image format was selected to be 1182 picture elements (pixels) wide by 1056 lines high. The encoding of this video data to seven bits, coupled with an 8.96 sec frame time produced a data rate of 2.112 megabits per sec. Improved sensitivity was achieved by employing a base-band signal chain as opposed to the chopped or carrier signal chain used in previous Mariner cameras. As a result of these improvements, the VIS represents a new generation in slow-scan vidicon cameras for planetary applications.

### General Description

The VIS consists of two identical, independently controlled and powered cameras and supporting electronics as presented in Fig. 1. The camera heads are mounted on a two-degree-of-freedom articulating platform attached to the Viking Orbiter. Each camera head is a composite device consisting of an optics assembly, a mechanical shutter, a six-position filter wheel, and a magnetically focused slow scan vidicon, and all associated electronics except the low-voltage power converter. A continuous VIS data stream is generated by reading out one camera while the second camera is being erased and exposed. VIS image data is converted to digital form and transferred to the flight data subsystem, where it is multiplexed with appropriate identification, synchronization, engineering data, and other science data to form a composite data stream. This composite data stream is then transferred to the data storage subsystem and stored on magnetic tape for subsequent playback at a rate commensurate with Orbiter communications link performance.

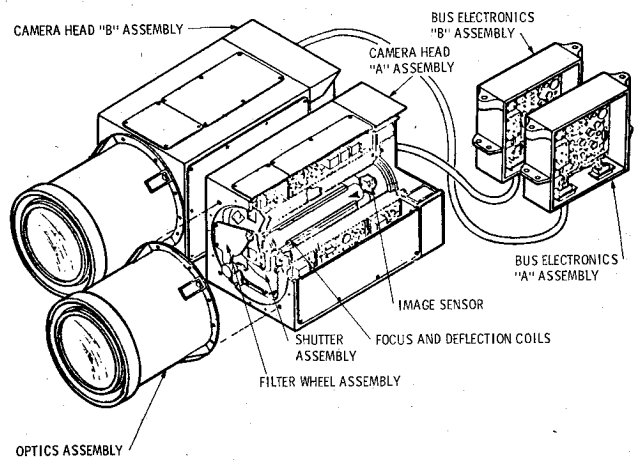


**Fig. 1 Visual Imaging Subsystem configuration.**

Presented as Paper 76-124 at the AIAA 14th Aerospace Sciences Meeting, Washington, D.C., Jan. 26-28, 1976; submitted March 11, 1976; revision received Aug. 2, 1976. This paper presents the results of one phase of research carried out at the Jet Propulsion Lab., California Institute of Technology, under Contract NAS 7-100, sponsored by the National Aeronautics and Space Administrator. The Langley Research Center is Project Manager for the overall Viking Project and is responsible for flight operations. JPL is responsible for the Orbiter; MMA is responsible for the Lander.

Index categories: Data Sensing and Presentation or Transmission Systems; Lunar and Interplanetary Spacecraft Systems, Unmanned.

*Member of the Technical Staff. Member AIAA.
†Supervisor, Advanced Imaging Development Group.
‡Manager, Space Instruments and Photography Section.
§Senior Scientist.

During normal operations both cameras are operating and the VIS data stream provides data for successive images every 4.48 sec. The VIS data rate is 2.112 Mbps.

Control of the VIS includes commandable selection of spectral filters, exposure duration, light flooding and amplifier gain. An exposure duration of zero is provided for special purposes such as sensor dark current determination, and to conserve wear on the shuttle during those times the cameras are on but not acquiring imaging data.

### Camera Operation

The operating sequence illustrated in Fig. 2 begins with the prepare cycle, which is divided into eight equal intervals. Vidicon light flooding is normally used to reduce the residual from the previous exposure. This occurs, when commanded, during the first of the eight intervals, and is accomplished by eight small incandescent bulbs arrayed around the rear of the shutter aperture, which expose the vidicon well beyond saturation. This interval is also used to reset the shuttle and to step the filter wheel, when commanded.

When exposure times of less than 420 msec are commanded, which is the case for all but star pictures, the next 6 time intervals are used to erase the vidicon photo surface. This is accomplished by increasing the line scan rate by a factor of 10 and the frame rate by 8. Scan size is also increased by about 10% to prevent edge effects in erasure. The number of scan lines per erase frame is increased to 1320, from the readout 1056, to avoid Moire effects between read and erase line patterns.

The eighth interval is used for exposure. Exposure time generation is derived digitally from the 300 kHz pixel clock transmitted to VIS from the spacecraft Flight Data Subsystem, and proceeds from 3.18 msec to 2.66 sec in a 4/3, 3/2, 4/3...progression. When exposures longer than 420 msec are commanded, the 4th thru 7th erase cycles are automatically inhibited and exposure starts with the 4th erase interval, ending at the time programed.

The readout cycle of each camera occupies the 4.48 second interval corresponding to the other camera's prepare cycle. Each of the 1056 line intervals is equal to 1280 pixel times, 76 of which are reserved for blanking and line retrace.

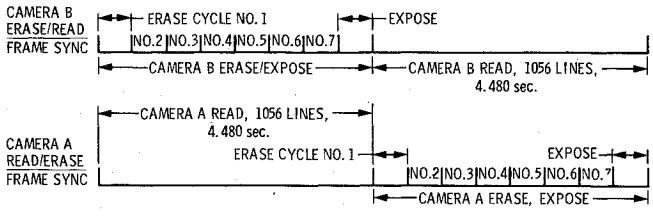


NOTE: 1. FOR EXPOSURE INTERVALS BETWEEN 420 m sec. AND 2660 m sec. ERASE CYCLES 4, 5, 6, AND 7 ARE INHIBITED BY VIS.

2. LIGHT FLOODING WHEN COMMANDED OCCURS DURING THE FIRST ERASE FRAME

**Fig. 2 Timing diagram.**

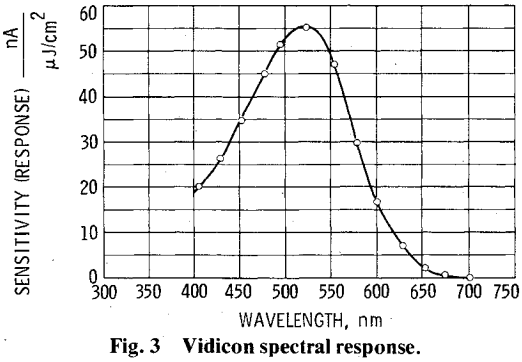


**Fig. 3 Vidicon spectral response.**

### Sensor

The sensor used in the VIS is a 1½″ diameter very high resolution slow scan vidicon, Westinghouse Type WX166, developed specifically for this application. It utilizes a D-type selenium sulfur photosurface material which has been doped to improve the long wavelength response. Typical photosurface response is shown in Fig. 3. Typical saturation photo current available from the tube is 50 nA. Residual current after light flooding to several times saturation, and six erasures, is 6 nA. This residual is reduced to about 4 nA by increasing the cathode to target voltage during erasure, the balance being removed in the signal chain.

### Optics

The telescope is an all spherical Schmidt-Cassegrain design employing a Mangin primary mirror, two full-aperture correctors and two field corrector elements, as shown in Fig. 4. Baffling is provided by the independently mounted sunshade. Optical performance is essentially diffraction limited, providing 70% response at the vidicon scan density of 42 line pairs per millimeter. This, combined with the vidicon response, yields an average square wave response, through the cameras, of 40% of 100 TV lines/picture height.

The filter wheel assembly contains six spectral filters including both absorptoin and interference types. By convolving the spectral transmission of the filters with the optics transmission, vidicon spectral sensitivity, and the spectral radiance of Mars, the spectral response shown in Fig. 5 was derived.

### Mechanisms

The shutter mechanism is a modification of previous Mariner shutters. Changes incorporated were a soft mount to

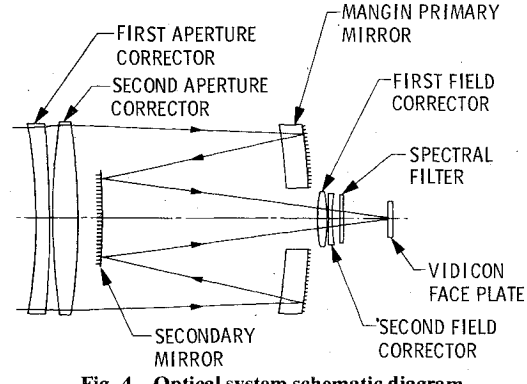


**Fig. 4 Optical system schematic diagram.**

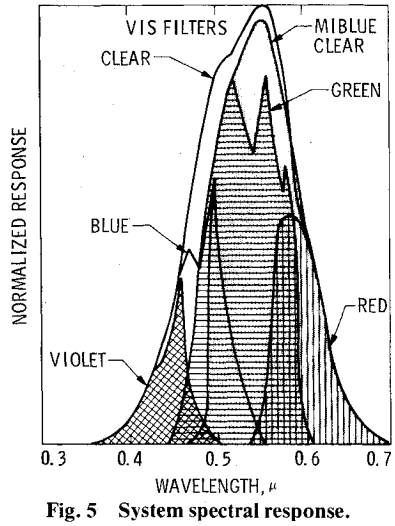


**Fig. 5 System spectral response.**

minimize shock coupling to the vidicon mesh, and addition of reinforcement to the rotor-drive arm assemblies to increase the life expectancy to 250,000 operations. The filter wheel assembly was redesigned for this mission to reduce the thickness of the shutter and filter wheel combination to the 1.6 in. available back focal distance. The design employs a true rotary solenoid located outside the diameter of the filter wheel. The prototype filter wheel was tested for its life expectancy of 100,000 cycles without significant wear.

#### Electronics

The camera electronics consists of about 1000 electronic parts per camera divided between the camera head and the auxiliary chassis located in the Viking Orbiter Bus. The auxiliary chassis contains the input power converter, which includes an input current limiter, main power transformer, three unregulated supplies, three regulated supplies, and the vidicon filament voltage and alignment current regulators. The camera head contains all remaining circuitry, including vidicon deflection circuits, signal chain, high voltage power supply, timing generator, data and timing interfaces, and auxiliary engineering measurement circuits.

## III. Camera Calibration

After several preliminary calibrations, producing reference data spanning a year's time, three sets of VIS measurements defining anticipated orbital performance were taken for four flight cameras and a spare during Dec.–Jan. 1974–1975. These data consist of a subsystem Bench calibration both before and after testing in a thermal vacuum chamber at 10°C, 20°C, and 30°C. A final verification of both spacecraft was also made at the Eastern Test Range (ETR) during May, 1975. In addition to numerous engineering tests, each calibration was designed to record the VIS light transfer and shading through all filter positions by varying shutter speeds for constant illumination, signal reciprocity with compensating shutter speed and source variation, and residual image, square wave response and point source imaging. Special tests were also performed to evaluated veiling glare, shutter light leak, frame to frame repeatability, and random and coherent noise contributions to image data. These tests and their results are described in detail in the "VO'75 VIS Calibration Report."[2]

#### Light Transfer

Figure 6 illustrates the four flight cameras' light transfer characteristics compared with the sensitivity of the Mariner 9 instruments for 200×200 element areas located near the centers of the fields view. The ability to change gain states results in an effective dynamic range of over 300 per filter. A linearity deviation of less than 2% is typical of measurements made in the high gain state.[3]

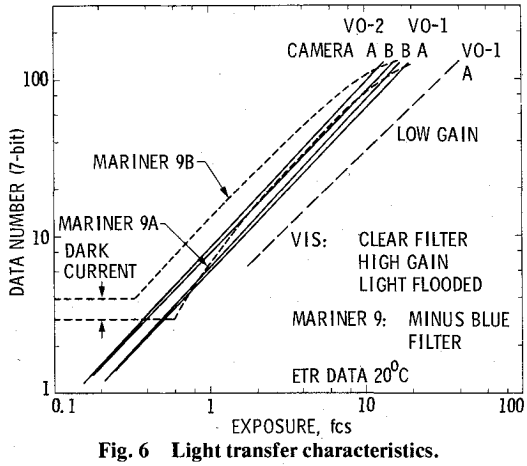


Fig. 6 Light transfer characteristics.

Accurate calibration of the camera response variation across the frame format (shading) is necessary to permit decalibration of the Mars images. Failure to adequately correct this vidicon artifact is manifested in the annoying changes in image tone across frame boundaries in image mosaics. A variation of nearly 10% in response is present over the entire picture format, primarily a result of shading in the light flood residual. Because the cameras exhibit remarkable frame-to-frame stability (0.3% variation in the sample means and dispersions for 200 successive pictures acquired by VO-2 camera A), it is anticipated that shading removal may be successfully accomplished as part of the digital image processing.

Nominal planetary photography uses light flooding to reduce the residual image from the previous picture. At the time of image readout, the flood residual (~0.4V) creates a background "pedestal" near 0 DN with a commandable offset on, or one-third scale DN (high gain state) with offset off. While shading is evident in this backgroind, the residual image from the previous frame is reduced to approximately 0.5%.

Reciprocity failure is noticeable in all camera pictures taken with short exposures. Figure 7 indicates an offset of approximately 1 msec between the commanded shutter speed and the actual focal plane exposure. Because the blades always travel in a vertical direction (opposite gravity), this measurement is not directly applicable to inflight (0 g) photography.

#### Resolution

The camera's spatial response alone does not adequately reflect the smallest Mars surface feature which might be iden-

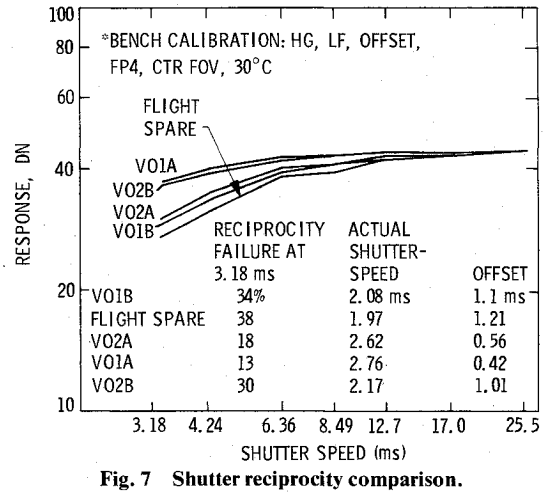


Fig. 7 Shutter reciprocity comparison.

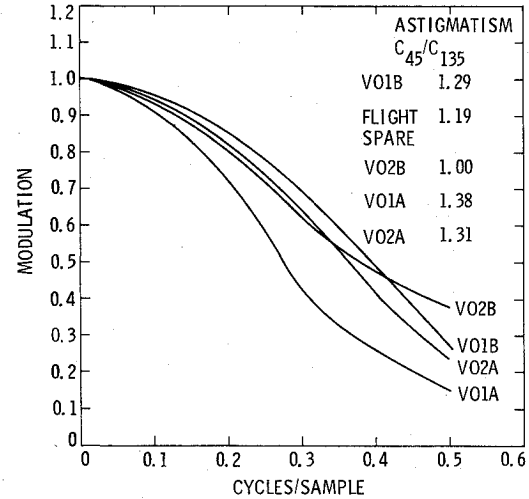


Fig. 8 MTF comparison.

tified. "Resolution" is dependent on the system Modulation Transfer Function (MTF) and high frequency random and coherent noise. Because the VIS cameras are focused for an expected operating temperature of 15°C, bench MTF calibaration (30°C) did not reveal the best instrument response at high spatial frequencies (Fig. 8). Figure 9 shows the effect of temperature on 1000 TV line response for all cameras. These data are inferred from measurement of the focal plane shift with temperature and the bench photography of slant bar targets. The utility of target modulations oriented at various angles to the image readout scans was demonstrated by the detection of astigmatism in the read beam. Hence, resolution at 45° to a TV line differs noticeably in some cameras from the highest image frequencies seen at 135° to this axis.

The high-frequency random noise background present in the electronic signal chain amounts to 0.7 DN in the high gain state or as much as 2 DN peak to peak. Hence, scene contrasts must produce low-frequency image modulations of at least 20 DN to obtain high-frequency responses corresponding to resolutions of ≤2.5 TV lines (100 m surface resolution at a periapsis attitude of 1500 km). Also present in typical images is coherent microphonic noise produced by the shuttering and shutter reset of the adjacent camera. A low amplitude coherent pattern may be observed near the top and bottom of processed images which have undergone strong contrast enhancement.

### Geometry

The consistency of image locations with the relative geometry of object space is of vital importance to photogrammetry of the landing sites. Total geometric distortions of VIS images were estimated by comparing known grid target locations with positions deduced from its television image. Typical residuals of up to 6–10 pixels across a frame are attributable to electronic effects. Once in flight, spatial dimensions may be estimated using the calibrated positions ($\pm 10^{-3}$) mm of 103 fiducial reseau marks present in the field of view. The image format as defined by the lines and samples is also slightly trapezoidal in appearance due to a small orthogonality error of ~1.0%.

The fields of view of each camera are offset by ±0.69° from the commanded instrument platform pointing direction (Fig. 10). The 1.69° × 1.54° field of view per camera then provides a 0.3° overlap in the image scan (clock angle) direction. A small twist angle also exists when comparing the reseau pattern horizontal axis with the mounting platform. This misalignment amounts to only 0.4°, however, for the worst case (VO-1 camera B).

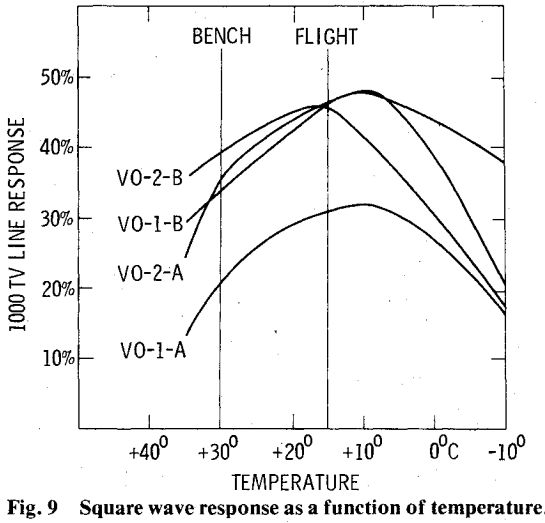


**Fig. 9 Square wave response as a function of temperature.**

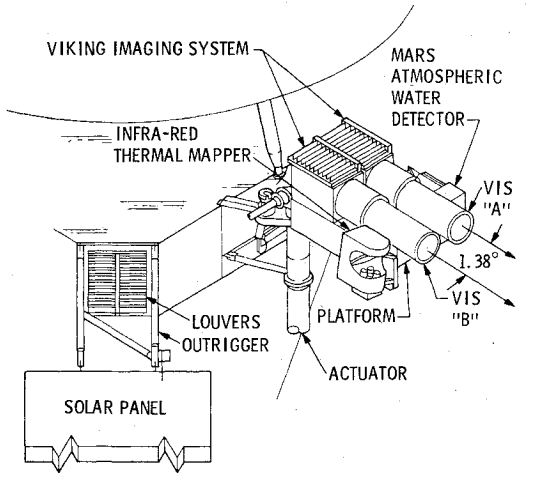


**Fig. 10 Scan platform with science instruments.**

## IV. Performance Prediction

Having discussed the measured response of the VIS to known stimuli, one can predict the performance of the cameras at Mars, using the known optical properties of Mars and the behavior of the Viking spacecraft in its orbit about the planet. The principal requirements to be satisfied relate to coverage of the surface, resolution, and accurate rendition of detail. Coverage is determined primarily by the field of view of the camera and the spacecraft-Mars-sun geometry. Determination of resolution in VIS images depends additionally on the shutter times used for exposure and the performance of the camera signal chain. For that reason the discussion of exposure prediction and resolution are intertwined.

### Coverage

Near periapsis, the projection of the VIS field of view on the planet (footprint) is 40 × 44 km. Considering that the surface area of Mars if $144 \times 10^6$ km$^2$, a simple calculation shows that at maximum resolution, 82,000 frames would be needed to cover the entire surface. Primarily because of the limitations of telemetry rates about 6000 frames are anticpated during the nominal orbital mission (June—Nov, 1976). It is clear that the Viking VIS will provide high resolution coverage only of selected targets of prime interest representing a small fraction of the planetary surface.

The Viking orbits are elliptical with 1500 km periapsis and 32,000 km apapsis. It is thus possible to make a choice between area covered and resolution attained by selecting the altitude at which the picture is acquired as shown in Fig .11. The size of the individual picture elements (pixels) is given as an approximate indication of resolution. For the high resolution end of the diagram, smear may be significant thus lowering the resolution from that shown.

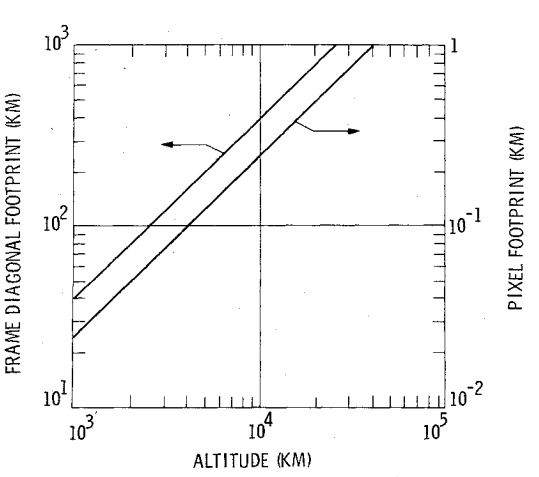


**Fig. 11 Pixel and frame-diagonal footprints.**

The observational sequence in which frames are acquired alternately from each camera with continuous data recording and no scan platform slewing is called a swath. In a typical case illustrated by Fig. 12 the coverage is redundant for large portions of the swath. As a result, the total area coverage is less than optimum. This redundancy results from the misalignment of the projection of the camera system line of symmetry with the spacecraft ground track.

A strip is an observational sequence in which frames are acquired alternately from each camera with continuous data recording and small scan platform slews between frames. A strip may be utlilzed at low altitude to produce more satisfactory area coverage than a swath. A typical strip centered on the same region of the planet is shown in Fig. 13. In contrast with a swath, the strip covers an area which is, in general, aligned in the cross-track direction.

The pentad is a special case of the strip sequence, consisting of the acquisition of five frames. The pentad can be utilized at high altitude to produce large area coverage as illustrated in Fig. 14.

**Exposure Prediction**

Obtaining the proper exposures for the images is considerably more important for this mission than it has been for previous missions. The use of seven bit encoding (Mariner 9 used nine bit encoding) limits the number of grey levels possible within a given image. For high resolution images of the Martian surface a scene modulation on the order of 15% is anticipated. Accordingly an image exposed near the middle of the encoding range will typically contain a span of DN values from 50 to 70 resulting in a maximum of twenty discrete grey levels in the image. An exposure time half as great would produce only ten discrete levels.

To deal with this situation it is necessary to define a display SNR. The display SNR is the ratio of the peak modulation in an image to its rms noise level. Based on computations of display SNR for each possible shutter time and gain setting a selection of the optimum settings is made. It is then possible to describe the surface resolution attainable for the frame. The calculation performed by a computer program proceeds along the lines described below.

The relationship between the incident light level and the encoded signal is governed by the light transfer characteristic described earlier (see Fig. 7). This characteristic may be modeled as

$$i = gAE^{\gamma} \tag{1}$$

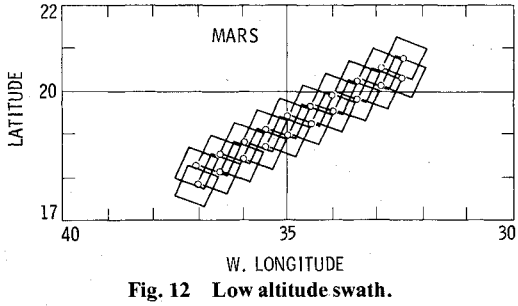


**Fig. 12 Low altitude swath.**

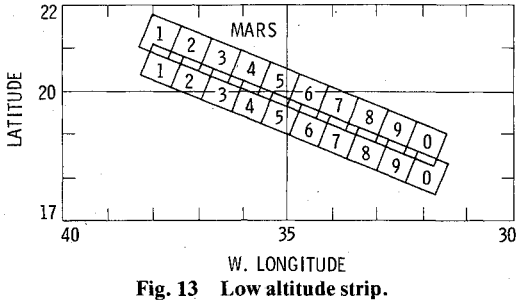


**Fig. 13 Low altitude strip.**

where $i$ is the signal in DN, $g$ is the gain coefficient, $A$ is the light transfer coefficient (camera sensitivity), $E$ is the exposure, and $\gamma$ is the slope of the linear region of the light transfer characteristic on a full logarithmic plot.

The camera optics transform the light reaching the camera into a spatial image on the vidicon photosurface. The photosurface, in turn, converts the optical image into a charge distribution which is read by the scanning electron beam in the vidicon. The modulation in the original scene is modified by the optics and vidicon in a manner characterized by the Modulation Transfer Function shown in Fig. 9. Image motion during shuttering also affects the spatial frequency response, thereby contributing its own smear MTF.

$$\text{MTF(smear)} = \sin n\pi f / n\pi f \tag{2}$$

where $n$ is the number of pixels of image smear, and $f$ is the spatial frequency. The total MTF is the convolution of these two contributing sources and is therefore a function of the shutter time.

Computation of the peak to peak signal modulations necessitates convolving the system MTF with the scene modulation. Certain types of natural scenes have been shown to exhibit power spectral densities which roll off at 20 dB/decade with frequency.[4] The Martian terrain, viewed from a low altitude spacecraft, exhibits such extreme degradation in contrast; however, those images require contrast enhancement by factors of from 5 to 10. Additionally the image processing includes high spatial frequency enhancement algorithms which significantly alter the image power spectrum. Recognizing the extreme interest in features of small spatial extent, a uniform scene modulation has been assumed in this computation. The validity of this assumption for the purpose of establishing optimum exposures will be tested by examination of the images from Mars orbit.

For each shutter time/gain state combination producing an exposure within the dynamic range of the VIS, the display signal to noise ratio curves are calculated by computer. A criterion value of 4 for the threshold display SNR is chosen which provides for some compromise between maximum resolution and maximum signal to noise. The frequency at which the display SNR equals the criterion value is determined iteratively. This frequency is converted to a resolution element dimension on the Martian surface. After each of the shutter time/gain state combinations has been examined, the one which produces the minimum resolution element on the surface *for the specified DSNR criterion* is selected as the optimum exposure setting.

When smear is negligible it is intuitively clear that the best exposure is the one which places the image histogram near full

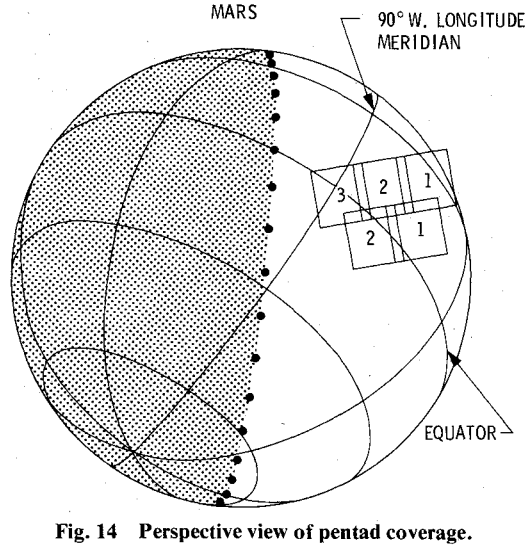


**Fig. 14 Perspective view of pentad coverage.**

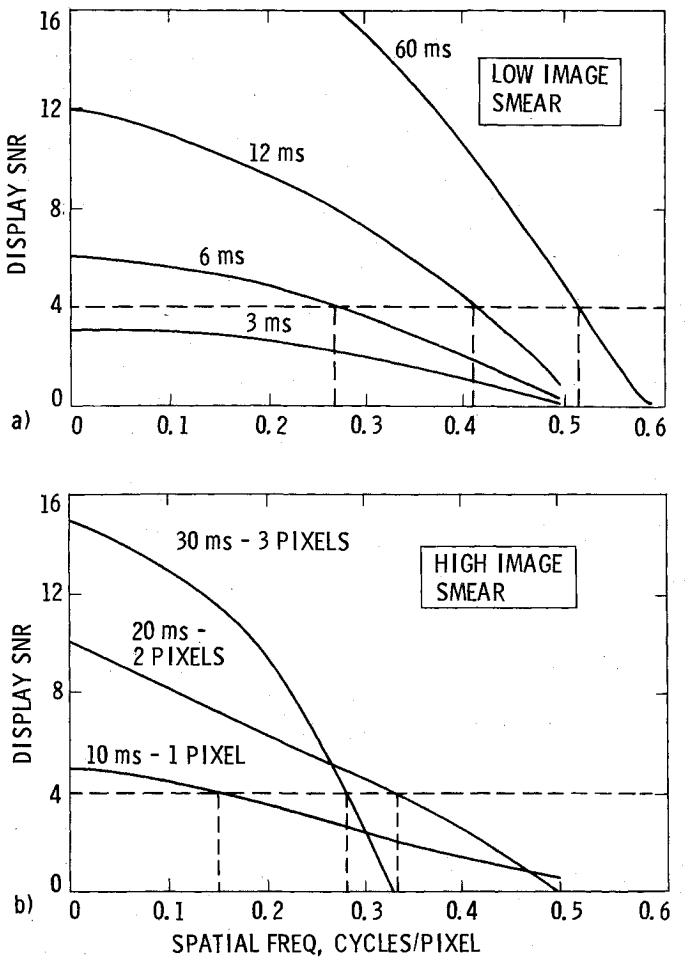


Fig. 15 Exposure optimization procedure. a) Low image smear. b) High image smear.

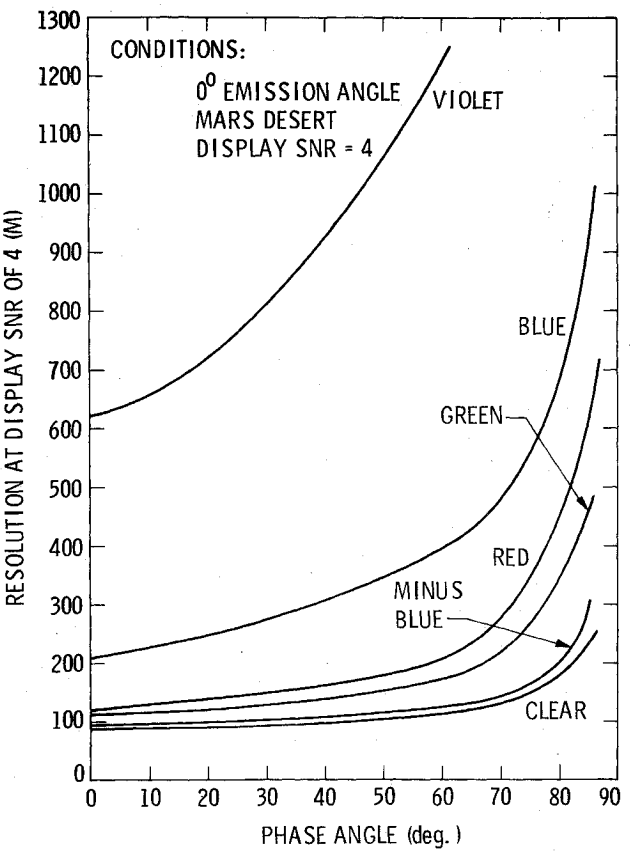


Fig. 16 Resolution at periapsis as a function of phase angle.

scale, thereby maximizing the signal to noise ratio at all spatial frequencies. This is shown in Fig. 15a. As exposure is increased the display SNR shifts higher at all spatial frequencies. By selecting the case which intersects the display SNR line at 4.0 (or at any reasonable constant value for that matter) the maximum exposure case is chosen (cases resulting in overexposure have been previously eliminated). It should be noted that for a 60 msec exposure in Fig. 15a, the display SNR curve intersects the criterion value at a spatial frequency higher than the Nyquist frequency (0.5 cycles/sample). This implies a resolution higher than the sampling theorem allows. As a result the predicted resolution is fictitious. This happens because the camera MTF is relatively high at the sampling frequency. Nonetheless, this exposure is preferable to the shorter exposures because the display SNR is higher for all frequencies below the sample rate. It has not been shown that the aliasing implied by finite response above the sampling rate causes any significant artifacts for natural scenes.

When smear is significant the problem is more difficult. As Fig. 15b indicates, an increase in shutter time increases the display SNR at low frequencies but lowers it at higher frequencies. The criterion of display SNR = 4.0 results in a selection of 20 msec shutter time and two pixels of smear. Had a display SNR of 8.0 been chosen for the criterion, a 30 msec exposure with 3 pixels of smear would have been selected.

There is no "correct" value for the criterion value of the display SNR. A value must be selected by making a judgment of the quality of the images received when the criterion is applied. The value of 4.0 would appear to be a reasonable value after reviewing smear simulations and the images from previous missions. The Viking mission profile includes an exposure test in the early orbital photographs for the purpose of obtaining images which represent different choices for the display SNR. An examination of these frames by the users has resulted in the choice of 8.0 for the value of the criterion display SNR.

#### Spatial Resolution

If smear resulting from image motion were not significant, VIS resolution capabilities could be stated quite simply as a function of spacecraft altitude. Since smear can be significant, the more elaborate exposure determination described above must be done prior to determining the resolution. The ultimate resolution is therefore affected by the smear velocity, illumination angle, choice of spectral filter, and optimization criterion.

Figure 16 illustrates the effects of phase angle and filter position on the resolution attainable at the nominal periapsis altitude of 1500 km. At phase angles greater than 60° where the illumination geometry provides the best distinguishability of surface relief, high resolution imaging will be confined to the use of clear and minus blue filters. At altitudes greater than 5000 km the effect of image smear is less significant, hence all of the spectral filters can be used. These limitations on camera utilization pose no major restrictions on the types of photographic sequences being planned. The major objective of the low altitude imaging is the acquisition of single color coverage of geologic features including sequences designed to produce convergent stereo image pairs. The primary use of multi-spectral images is scheduled for high altitude sequences in which a larger portion of the planet may be imaged in multiple colors without consuming large portions of the picture budget.

## V. Results of In-Flight Photography

The Viking cameras have now been subjected to a series of in-flight calibrations and, at the time of this writing, have acquired in excess of 700 pictures of the Martian surface from

**Table 1 Star sensitivity**

| Camera: | VO-1A | VO-1B | VO-2A | VO-2B |
|---|---|---|---|---|
| Predicted visual threshold magnitude (SNR = 7)[a] | 7.5 ± 0.2 | 8.1 ± 0.2 | 7.9 ± 0.2 | 8.3 ± 0.2 |
| Stars detected (SNR) | +5.9 (23) | +6.9 (22) | +5.9 (23) | +6.9 (20 |
| | +8.0 (4.0) | 6.9 (10) | +8.0 (4.6) | 6.9 (14) |
| | +7.5 (4.4) | +8.3 (3.4) | +7.5 (6.7) | +8.3 (3.8) |
| | +7.8 (6.9) | | +7.8 (10.7 | |
| | +7.9 (3.3) | | +7.9 (4.6) | |
| | +8.4 (2+7) | | +8.4 (4.9) | |
| | +8.5 (1.14) | | | |

[a]Signal to random noise ratio to background. Stars located in pictures taken Oct. 9 and 13, 1975, during inflight instrument checkout.

orbit. Detailed discussion of these images will be reported subsequent to this paper. The general conclusions regarding camera performance are summarized in the following.

Sensitivity of the cameras was verified by the examination of star images. Table 1 lists the predicted star sensitivities of the camera, and the visual magnitudes of the stars detected in the images. In a technique similar to that used for the analysis of the Mariner 10 camera resolution,[5] calibration images of pinhole targets were compared to the star images to verify that the VIS point response functions had not changed from preflight values.

Images of both Jupiter and Mars were acquired during cruise for the purpose of verifying the VIS light transfer curves shading and filter factors. Changes in the light flood residual correlated with the change in VIS operating temperature has been observed. Changes in the camera shading has also been observed. A new set of shading correlation data has been generated for use in decalibrating the orbital data.

Shortly after the Viking spacecraft was inserted into Martian orbit, an exposure test sequence was performed to evaluate the exposure prediction strategy described earlier in the paper. Using the results of these observations and other orbital photography, minor revisions to the exposure prediction data base were computed. The photography attained thus far has confirmed the validity of the camera calibration and performance predictions described here and has been used extensively in the selection of the landing site for Viking 1.

## References

[1]Carr, M.H., Baum, W.A., Briggs, G.H., Masursky, H., Wise, D.W., and Montgomery, D.R., *Icarus,* Vol. 16, Feb. 1972, pp. 17-33.

[2]Viking Orbiter 1975 Visual Imaging Subsystem Calibration Document, Jet Propulsion Lab., Pasadena, Calif., JPL Document 611-125.

[3]Thorpe, T.E., *Icarus,* Vol. 27, 1976.

[4]Cohen, P.W., Gorog, I., and Carlson, C.R., Technical Report, Office of Naval Research, Rept. PRRL-75-CR-2, Task NR-213-120, March 1975.

[5]Thorpe, T.E., "Mariner 10 Star Photography," *Journal of Spacecraft and Rockets,* Vol. 12, May 1975, pp. 314-317.